Pergamon

Int. J. Heat Mass Transfer. Vol. 37, No. 4, pp. 647–657, 1994
Elsevier Science Ltd

0017–9310/94 $6.00 + 0.00

Analytic formulae for the effective conductivity of a square or hexagonal array of parallel tubes

R. D. MANTEUFEL
Southwest Research Institute, 6220 Culebra Rd., San Antonio, TX 78238-5166, U.S.A.

and

N. E. TODREAS
Massachusetts Institute of Technology, 77 Massachusetts Ave., Cambridge, MA 02139, U.S.A.

(*Received* 5 *January* 1993 *and in final form* 27 *July* 1993)

Abstract—A set of analytic formulae are presented for the effective thermal conductivity of either a square or a hexagonal array of parallel tubes which have distinct core, tube and fill conductivities. The formulae are based on a generalization of Rayleigh's [*Phil. Mag.* **34**(5), 481–502 (1892)] method to include hexagonal (as well as square) arrays, tubes (as well as solid rods), and higher-order terms in the analytic series. The accuracy of the analytic formulae is determined by comparison with essentially exact numerical calculations. The formulae are applied to the problem of an array of dry, spent, nuclear fuel rods.

INTRODUCTION

THE PURPOSE of this paper is to present and numerically validate a set of analytic formulae for the effective thermal conductivity, k_{eff}, of either a square or hexagonal array of tubes, see Figs. 1 and 2, respectively. Each tube consists of a core and tube wall with conductivities k_{core} and k_{tube}. When the core and wall are the same material, then the tube is a solid rod, k_{rod}. The region between the tubes is filled with a third material, k_{fill}. The arrays are assumed infinite so boundaries are not considered. The effective conductivity of interest is perpendicular to the array of tubes which appear as circles in a two-dimensional sketch. The effective conductivity is the conductivity value for which a homogeneous medium will exhibit the same heat transfer characteristics (i.e. the same heat flux for equal temperature gradients).

The set of analytic formulae extend and improve the range of available analytical solutions for the effective conductivity of a regular array of tubes. It is considered theoretically important to have this type of analytical solution for such a well defined class of problems. For example, the equations offer analytic solutions which can be used to benchmark computer codes (although properly implemented numerical solutions can be more accurate than the analytic formulae, especially as the accuracy of the numerical technique is increased). The analytic formulae also have the significant advantage of being easy to use because they do not require a computer program.

A motivation for this work stems from the need to calculate the k_{eff} for a dry spent nuclear fuel assembly which consists of fuel rods in a regular pattern (either square or hexagonal array). During transportation and dry storage, the fuel assemblies are placed in an air-tight container which has an essentially stagnant fill gas. The fuel rods consist of a center core (fuel) and a tube wall (clad) as illustrated in either Fig. 1 or 2. Spent fuel rods have a fuel-to-clad gap thermal resistance which is discussed later in this paper.

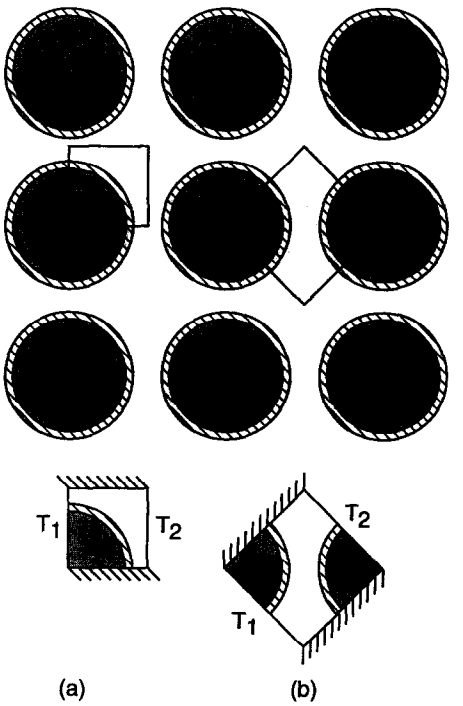

FIG. 1. Square array of tubes with computational domains used to calculate the conduction factor, F_{cond}, in the (a) horizontal and (b) 45 degree direction.

NOMENCLATURE

a, b, d, D, v	coefficients in formulae (no names)	k_{eff}	effective conductivity
f	rod (or tube) volume fraction	k_{fill}	fill conductivity
$f_{\max}$	maximum volume fraction (rods touching)	k_{rod}	rod conductivity (for solid rod only)
F_{cond}	conduction factor, $k_{\text{eff}}/k_{\text{fill}}$	k_{tube}	tube wall conductivity (for tube only)
HX	hexagonal array	r_o	outer tube radius
k_{core}	core conductivity (for tube only)	r_i	inner tube (outer core) radius
		SQ	square array
		t	tube wall thickness, $r_o - r_i$.

BACKGROUND LITERATURE

The problem of heat conduction perpendicular to an array of tubes has many mathematical analogies to phenomena in materials [1–3], optics [4–7], biology [8], electrical conductivity [9–11], vibration [9] and mathematics [12–15]. A complete presentation of the mathematical analogies is beyond the scope of this paper, hence this paper concentrates on the effective thermal conductivity.

There have been many articles published on the effective conductivity of a regular array of tubes or solid rods. Only the most important background articles will be discussed in this work. The basic method for solid rods is outlined by Rayleigh [9]; extended to tubes having the same core material as the fill material by Runge [10]; generalized by Keller's reciprocal theorem [11, 12]; extended to tubes having a core material different from the fill material by Israelachvili *et al.* [4, 5] and by Ninham and Sammut [8]; and extended to hexagonal arrays by Perrins *et al.* [7]. This paper combines and extends the earlier results, with emphasis on tubes (as well as solid rods), within hexagonal (as well as square) arrays, and increases the number of terms retained in the analytic series.

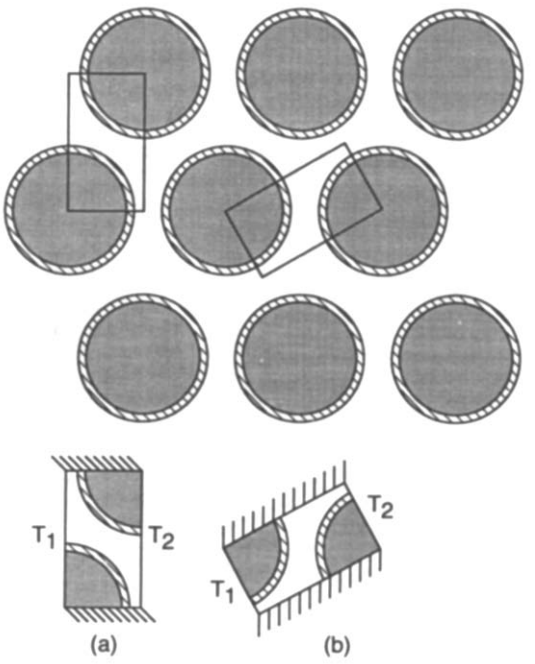

FIG. 2. Hexagonal array of tubes with computational domains used to calculate the conduction factor, F_{cond}, in the (a) horizontal and (b) 30 degree direction.

Lord Rayleigh [9] published a seminal article where he considered the electrical conductivity, refractive index and relative density of a composite medium consisting of either solid rods in a square array or solid spheres in a cubic array. Rayleigh's original theoretical approach continues to be useful and has not been outdated or replaced (although alternative methods have been developed for tightly-packed, highly-conductive cylinders [15]). Because of its length and mathematical complexity, Rayleigh's method is summarized in Appendix A, as it has been used to derive the expanded set of analytic formulae presented in this paper.

Runge [10] was the first to extend Rayleigh's method to the problem of tubes where the core of the tube was filled with the same material as the fill medium ($k_{\text{core}} = k_{\text{fill}}$). Although Runge states that the new formulae are valid only for thin tubes, we found the equations to be accurate for all tube wall thicknesses.

Keller [11, 12] presented the reciprocal theorem which is applied here to state that the conduction factor, $F_{\text{cond}} = (k_{\text{eff}}/k_{\text{fill}})$, for a given volume fraction, f(=volume fraction occupied by solid rod (or core plus tube)), and rod-to-fill conductivity ratio, $k_{\text{rod}}/k_{\text{fill}}$, is equal to the reciprocal of F_{cond} based on the same f and reciprocal $k_{\text{rod}}/k_{\text{fill}}$.

$$F_{\text{cond}}\left(f, \frac{k_{\text{rod}}}{k_{\text{fill}}}\right) = \frac{1}{F_{\text{cond}}\left(f, \frac{k_{\text{fill}}}{k_{\text{rod}}}\right)}. \tag{1}$$

In this paper, Keller's reciprocal theorem is used to confirm the numerical calculations.

Israelachvili *et al.* [4, 5] and Ninham and Sammut [8] present formulae for arrays of tubes with three distinct material conductivities (k_{core}, k_{tube} and k_{fill}). Although brief, the paper by Israelachvili *et al.* [4] does reveal considerable investigation to include the effects of tubes with different core, wall and fill con-

ductivities. It should also be noted that two typographical errors were found in the paper by Ninham and Sammut [8]. In their equation (5), the number 0.133 should be 0.0133615 and in their equation (83), the exponent on a^m should be a^{2n}. Israelachvili is acknowledged by Ninham and Sammut [8] as contributing important comments to their paper where it appears that Israelachvili highlighted his earlier work to extend Rayleigh's and Runge's equations from solid rods to tubes. Both groups, however, only considered a square array.

Perrins *et al.* [6, 7] present an extension of Rayleigh's method to a hexagonal array of solid rods. Perrins *et al.* [6] noted that Rayleigh omitted a term in an equation for the square array of solid rods (in Table 1 of this paper, the term $b_{8\text{-}1}f^8v_3v_5$ was missing from the 4th & 5th order solution for the square array in Rayleigh's paper). Perrins *et al.* conclude that Rayleigh used a 'triangular truncation' of the terms in the analytic expansion. However, Rayleigh's equation is actually based on a 'linear truncation'. This difference was not considered significant by Perrins *et al.*, nor is it here (although our equations do include this term). A slight typographical error was also found in Perrins *et al.*'s [6] work: in their Appendix 1, equation (A1.5) the S_6, S_{18}, S_{30}, ... sums are shown to have negative values, however all of the S sums are positive values. Their final equations and calculations do agree with our work. Perrins *et al.* only consider solid rods, however, and the work was not generalized to include tubes.

ANALYSIS

The results of this work are presented in dimensionless form for greater generality. The primary quantity to be calculated is the conduction factor, F_{cond}, which is defined as:

$$F_{cond} = \frac{k_{eff}}{k_{fill}}. \tag{2}$$

The term 'effective conductivity' is used in this work where 'conduction factor' is more exact. For example, the analytic formulae are written in terms of F_{cond} and not k_{eff}. However, formulae for the 'effective conductivity' are more easily understood so that term is used freely here.

Five dimensionless parameters are used to express the conduction factor as a function of (i) array pattern (i.e. either square, *SQ* or hexagonal, *HX*), (ii) volume fraction, (iii) core-to-fill conductivity ratio, (iv) tube-to-fill conductivity ratio, and (v) inner-to-outer radius ratio. In summary, the functionality for an array of tubes is:

$$F_{cond} = F_{cond}\left(\{SQ \text{ or } HX\}, f, \frac{k_{core}}{k_{fill}}, \frac{k_{tube}}{k_{fill}}, \frac{r_i}{r_o}\right) \tag{3}$$

and for an array of solid rods is:

$$F_{cond} = F_{cond}\left(\{SQ \text{ or } HX\}, f, \frac{k_{rod}}{k_{fill}}\right). \tag{4}$$

Numerical calculations

The analytical formulae are compared with the results of numerical calculations. The numerical calculations are described by Manteufel [16] and are summarized in Appendix B. A properly implemented numerical method can yield results which are more accurate than the analytic formulae because the formulae are based on a truncation of an infinite series. However, analytic formulae have advantages such as being easier to use than a method requiring a computer program. The numerical results were found to be essentially exact (to approximately 5 digits) and were used to check the accuracy of the analytic formulae.

Analytic formulae

The analytic formulae were derived using Rayleigh's method and are summarized in Table 1. For each array, four different truncation orders are reported, i.e. the {1st, 2nd & 3rd, 4th & 5th, 6th & 7th} orders for the square array and the {1st & 2nd, 3rd & 4th & 5th, 6th & 7th & 8th, 9th & 10th & 11th} orders for the hexagonal array. The precise meaning of the integer grouping for the orders can be understood by following Rayleigh's method which is discussed in Appendix A. The higher order indicates more terms were retained in the infinite series. The most complex equations (6th & 7th order for the *SQ* array, and 9th & 10th & 11th order for the *HX* array) have not been previously published.

The lowest order formulae for the *SQ* (1st) and *HX* (1st & 2nd) arrays yield the same result (i.e. terms = 0 in Table 1) so that the F_{cond} is:

$$F_{cond} = \frac{1-fv_1}{1+fv_1}. \tag{5}$$

Equation (5) is a very simple formula and is considered accurate for many applications. When the rod conductivity (or equivalently the core and tube conductivities) is near the fill conductivity, then equation (5) is accurate. As the conductivity ratios increase, then the error increases.

For the special case of solid rods ($k_{core} = k_{tube}$), the parameter $d_{tube\text{-}core} = 0$, so that the formula for v_n reduces to (from Table 1):

$$v_n = \delta_{fill\text{-}rod} = \frac{k_{fill}-k_{rod}}{k_{fill}+k_{rod}}. \tag{6}$$

In this case, all of the v's are equal (i.e. $v_1 = v_3 = v_5 = \ldots$). Equation (6) is consistent with the solid rod equations published by Rayleigh [9] and Perrins *et al.* [6, 7].

Another special case is for tubes having the same core and fill material ($k_{core} = k_{fill}$), so that

Table 1. Summary of analytic formulae for the effective conductivity of a square or hexagonal array of tubes

$$F_{\text{cond}} \equiv \left(\frac{k_{\text{eff}}}{k_{\text{fill}}}\right) = \frac{1 - fv_1 - \text{terms}}{1 + fv_1 - \text{terms}} = 1 - \frac{2fv_1}{1 + fv_1 - \text{terms}}$$

SQ = square array	HX = hexagonal array
Volume fraction:	Volume fraction:
$f = \dfrac{\pi}{4(p/d)^2}$	$f = \dfrac{\pi}{2\sqrt{(3)}(p/d)^2}$
1st order: terms = 0	1st & 2nd order: terms = 0
2nd & 3rd order: terms = $a_4 f^4 v_1 v_3$	3rd, 4th & 5th order: terms = $a_6 f^6 v_1 v_5$
4th & 5th order: terms = $a_4 f^4 v_1 v_3/(1 - b_{8\text{-}1} f^8 v_3 v_5) + a_8 f^8 v_1 v_7$	6th, 7th & 8th order: terms = $a_6 f^6 v_1 v_5/(1 - b_{12\text{-}1} f^{12} v_5 v_7) + a_{12} f^{12} v_1 v_{11}$
6th & 7th order: terms = $a_4 f^4 v_1 v_3/D_4 + a_8 f^8 v_1 v_7 + a_{12} f^{12} (v_1)^2 + a_{16} f^{16} v_1 v_3 v_5 v_7/D_{16} + a_{20} f^{20} v_1 v_5 (v_7)^2/D_0 + a_{28} f^{28} v_1 v_3 (v_5)^2 (v_7)^2/D_{28}$	9th, 10th & 11th order: terms = $a_6 f^6 v_1 v_5/D_6 + a_{12} f^{12} v_1 v_{11} + a_{18} f^{18} (v_1)^2 + a_{24} f^{24} v_1 v_5 v_7 v_{11}/D_{24} + a_{30} f^{30} v_1 v_7 (v_{11})^2/D_0 + a_{42} f^{42} v_1 v_5 (v_7)^2 (v_{11})^2/D_{42}$
where:	where:
$D_0 = 1 - b_{12\text{-}1} f^{12} v_5 v_7$	$D_0 = 1 - b_{18\text{-}1} f^{18} v_7 v_{11}$
$D_4 = 1 - b_{8\text{-}1} f^8 v_3 v_5/D_0 - b_{12\text{-}2} f^{12} v_3 v_9$	$D_6 = 1 - b_{12\text{-}1} f^{12} v_5 v_7/D_0 - b_{18\text{-}2} f^{18} v_5 v_{13}$
$D_{16} = 1 - b_{8\text{-}1} f^8 v_3 v_5/D_0 - [b_{12\text{-}1} v_5 v_7 + b_{12\text{-}2} v_3 v_9] f^{12} + b_{20\text{-}1} f^{20} v_3 (v_5)^2 v_7/D_0 + b_{24\text{-}1} f^{24} v_3 v_5 v_7 v_9$	$D_{24} = 1 - b_{12\text{-}1} f^{12} v_5 v_7/D_0 - [b_{18\text{-}1} v_7 v_{11} + b_{18\text{-}2} v_5 v_{13}] f^{18} + b_{30\text{-}1} f^{30} v_5 (v_7)^2 v_{11}/D_0 + b_{36\text{-}1} f^{36} v_5 v_7 v_{11} v_{13}$
$D_{28} = 1 - b_{8\text{-}1} f^8 v_3 v_5/D_0 - [2b_{12\text{-}1} v_5 v_7 + b_{12\text{-}2} v_3 v_9] f^{12} + 2b_{20\text{-}1} f^{20} v_3 (v_5)^2 v_7/D_0 + [2b_{24\text{-}1} v_3 v_5 v_7 v_9 + b_{24\text{-}2} (v_5)^2 (v_7)^2] f^{24} - b_{32\text{-}1} f^{32} v_3 (v_5)^3 (v_7)^2/D_0 - b_{36\text{-}1} f^{36} v_3 (v_5)^2 (v_7)^2 v_9$	$D_{42} = 1 - b_{12\text{-}1} f^{12} v_5 v_7/D_0 - [2b_{18\text{-}1} v_7 v_{11} + b_{18\text{-}2} v_5 v_{13}] f^{18} + 2b_{30\text{-}1} f^{30} v_5 (v_7)^2 v_{11}/D_0 + [b_{36\text{-}1} v_5 v_7 v_{11} v_{13} + b_{36\text{-}2} (v_7)^2 (v_{11})^2] f^{36} - b_{48\text{-}1} f^{48} v_5 (v_7)^3 (v_{11})^2/D_0$
constants:	constants:
$a_4 = 0.305828$	$a_6 = 0.0754222$
$a_8 = 0.0133615$	$a_{12} = 0.000076500$
$a_{12} = 0.000184643$	$a_{18} = 0.0000000517088$
$a_{16} = 0.242252$	$a_{24} = 0.00423258$
$a_{20} = 0.0341942$	$a_{30} = 0.0000560053$
$a_{28} = 0.0479731$	$a_{42} = 0.0000593815$
$b_{8\text{-}1} = 1.40296$	$b_{12\text{-}1} = 1.06028$
$b_{12\text{-}1} = 2.55915$	$b_{18\text{-}1} = 0.73210$
$b_{12\text{-}2} = 0.15233$	$b_{18\text{-}2} = 0.0447964$
$b_{20\text{-}1} = 3.59039$	$b_{30\text{-}1} = 0.776234$
$b_{24\text{-}1} = 0.389837$	$b_{36\text{-}1} = 0.0327954$
$b_{24\text{-}2} = 6.54926$	$b_{36\text{-}2} = 0.535971$
$b_{32\text{-}1} = 9.18835$	$b_{48\text{-}1} = 0.568281$
$b_{36\text{-}1} = 0.997652$	

$$v_n = (\delta_{\text{fill-tube}} + \delta_{\text{tube-core}} (r_i/r_o)^{2n})/(1 + \delta_{\text{fill-tube}} \delta_{\text{tube-core}} (r_i/r_o)^{2n})$$
$$\delta_{\text{fill-tube}} = (k_{\text{fill}} - k_{\text{tube}})/(k_{\text{fill}} + k_{\text{tube}})$$
$$\delta_{\text{tube-core}} = (k_{\text{tube}} - k_{\text{core}})/(k_{\text{tube}} + k_{\text{core}})$$

the $d_{\text{tube-core}} = -d_{\text{fill-tube}}$, and the formula for v_n reduces to (from Table 1):

$$v_n = \frac{\delta_{\text{fill-tube}} \left(1 - \left(\frac{r_i}{r_o}\right)^{2n}\right)}{\left(1 - (\delta_{\text{fill-tube}})^2 \left(\frac{r_i}{r_o}\right)^{2n}\right)} \tag{7}$$

which is consistent with the results of Runge [10].

Directional F_{cond}

In general, the conductivity of a heterogeneous medium can be expressed using a symmetric second-order tensor. For a square or hexagonal array, the second order tensor is rotationally invariant because each is physically symmetric for either 90 (square) or 60 (hexagonal) degree rotations. Therefore, the effective conductivity is isotropic and can be expressed as purely a scalar quantity (i.e. proportional to the

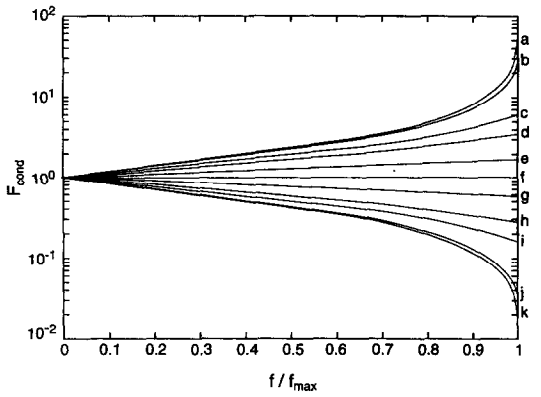

FIG. 3. Conduction factor calculated for solid rods in a square array for a range of rod-to-fill conductivity ratio, k_{rod}/k_{fill} = {1000(a), 100(b), 10(c), 5(d), 2(e), 1(f), 1/2(g), 1/5(h), 1/10(i), 1/100(j), 1/1000(k)}.

identity tensor) (see also refs. [6, 9]). This property was used to verify the numerical implementation by calculating F_{cond} in each direction (see Figs. 1 and 2). The results verified a correct implementation of the numerics.

Keller's reciprocal theorem

The accuracy of the numerical calculations was confirmed by comparison with Keller's reciprocal theorem [12] (see equation (1)), and the results are presented in Fig. 3. In Fig. 3, F_{cond} is numerically calculated for eleven values of k_{rod}/k_{fill} for rods in a square array. The error was defined as: Error = $1-F_{cond}(f, k_{rod}/k_{fill})\ F_{cond}(f, k_{fill}/k_{rod})$ and was found to be between 10^{-3} and 10^{-7} over the range of f/f_{max} for $10^{-3} \leqslant k_{rod}/k_{fill} \leqslant 1000$. This agreement confirms a correct implementation of the numerical algorithms.

Calculations for solid rods

The analytic formulae and numerical calculations for solid rods are compared in Figs. 4 and 5, for six values of k_{rod}/k_{fill}. The numerical calculations of F_{cond} are plotted as solid lines and are the same for the four plots. The analytic formulae are plotted as dashed lines where the order of the formulae is different for each plot.

The numerical calculations are considered accurate and essentially 'exact' to approximately 5 digits of accuracy of F_{cond}. It is noted that the analytic formulae

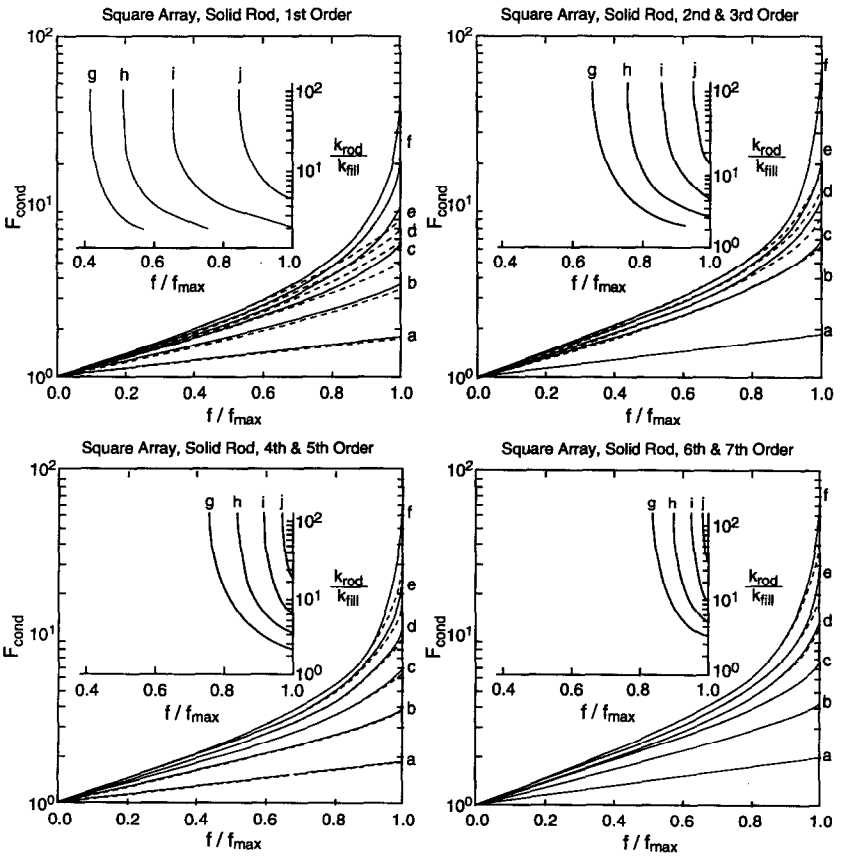

FIG. 4. Comparison of numerically calculated conduction factors (solid lines) with the analytic formulae (dashed lines) for a square array of solid rods for different rod-to-fill conductivity ratio, k_{rod}/k_{fill} = {2(a), 5(b), 10(c), 20(d), 50(e), 10000(f)}. The percent error contours {0.01%(g), 0.1%(h), 1.0%(i), 10.0%(j)} are shown in the upper-left sub-plots.

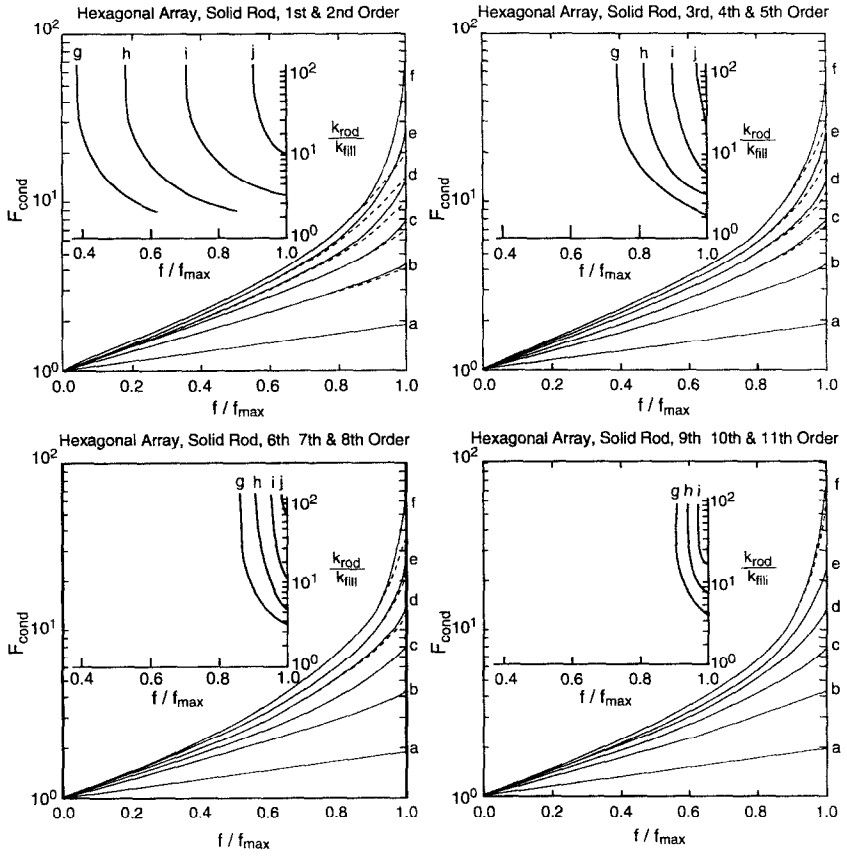

FIG. 5. Comparison of numerically calculated conduction factors (solid lines) with the analytic formulae (dashed lines) for a hexagonal array of solid rods for different rod-to-fill conductivity ratio, $k_{rod}/k_{fill} = \{2(a), 5(b), 10(c), 20(d), 50(e), 10000(f)\}$. The percent error contours $\{0.01\%(g), 0.1\%(h), 1.0\%(i), 10.0\%(j)\}$ are shown in the upper-left sub-plots.

consistently agree with the numerical calculations at low values of f, and improve in accuracy as the order of the formula is increased. The analytic formulae increasingly underestimate the numerical calculations both as f increases and as k_{rod}/k_{fill} increases. When k_{rod}/k_{fill} is close to unity, the analytic formulae provide accurate predictions over the entire range of f. For example, when $k_{rod}/k_{fill} = 2$, the numerical calculations (solid lines) and analytic formulae (dashed lines) are coincident, hence they appear as only a solid line.

Error contours are shown as sub-plots in the upper-left corner of Figs. 4 and 5. From these error contours, one can identify where a given analytic formula is within 0.01, 0.1, 1.0 and 10% of the exact solution (where the numerical calculations are assumed to be the exact solution). For example, one can read from Fig. 4(a) that the 1st order analytic formula is within 1% for isothermal rods ($k_{rod}/k_{fill} \gg 1$) up to $f/f_{max} = 0.54$ (or equivalently $f = 0.420$, because $f_{max} = 0.7854$). Similarly, from Fig. 5(b) the 2nd & 3rd order analytic formula is within 1% for isothermal rods up to $f/f_{max} = 0.83$ ($f = 0.653$). As previously noted, isothermal rods represent the worst case for underestimating the solution, so that for finite conductivity rods or tubes, the analytic formulae are accurate up to greater values of f.

For comparison purposes, the volume fractions at which the error is greater than 1% are reported in Tables 2 and 3 for each of the analytic formulae.

Table 2. Volume fractions for the analytic (formula to be accurate within one percent (1%) for a square array of isothermal (i.e. infinite conductivity) solid rods

Order	1st	2nd & 3rd	4th & 5th	6th & 7th
f/f_{max}	0.537	0.831	0.905	0.941
f	0.420	0.653	0.710	0.739

Note: $f_{max} = \pi/4 \cong 0.7854$ for square array.

Table 3. Volume fractions for the analytic formula to be accurate within one percent (1%) for a hexagonal array of isothermal (i.e. infinite conductivity) solid rods

Order	1st & 2nd	3rd, 4th & 5th	6th, 7th & 8th	9th, 10th & 11th
f/f_{max}	0.696	0.889	0.951	0.968
f	0.631	0.807	0.863	0.878

Note: $f_{max} = \pi/(2\sqrt{3}) \cong 0.9069$ for hexagonal array.

As expected, the higher order formulae are accurate, however, they are more complex (see Table 1). Also, the percent improvement in accuracy decreases as each additional term is added. Hence the equation complexity greatly increases while the improvement in accuracy only slightly improves.

It is noted that for many practical problems, k_{rod}/k_{fill} will not be a large number and the simplest formula (equation (5)) is accurate for a significant range of f.

Calculations for tubes with $k_{core} = k_{fill}$

The accuracy of the analytic formulae was checked for the special case of tubes whose cores contain the fill as noted in equation (7). The calculations were performed for both square and hexagonal arrays for varying tube wall-thickness-to-outer-radius ratio, t/r_o. Only a small portion of the results (SQ array, three values of t/r_o) are presented in Fig. 6 as representative of the tube calculations. In Fig. 6, the formulae are plotted as solid lines and the numerical calculations as circles. The analytic formulae are consistently accurate and improve in accuracy as t/r_o decreases.

Calculations for spent nuclear fuel

The original motivation for this work was to calculate the k_{eff} for a dry spent nuclear fuel assembly. An assembly is typically described as either a square array (for boiling water or pressurized water reactor assemblies) or a hexagonal array (for consolidated or liquid metal reactor assemblies). An assembly consists of fuel rods which have a center core (UO_2 fuel) and cladding (tube wall, commonly zircaloy). During transportation and dry storage, the spent fuel assemblies are placed in an air-tight container, then vacuum pumped and backfilled with a non-oxidizing gas such as helium (He) or nitrogen (N_2). The fill gas remains essentially stagnant. Numerical calculations were performed for the nominal case of UO_2 fuel ($k_{UO_2} = 5$ W m^{-1} °C^{-1}), zircaloy clad ($k_{zircaloy} = 15$ W m^{-1} °C^{-1}), either nitrogen ($k_{N_2} = 0.04$ W m^{-1} °C^{-1}) or helium ($k_{He} = 0.2$ W m^{-1} °C^{-1}) fill, and in either a square or a hexagonal array. The length ratios are representative of a PWR assembly (from ref. [16]; $d = 0.95$ cm, $t = 0.056$ cm).

Between the UO_2 fuel and the tube cladding, there exists a gap which is filled primarily with gaseous fission products (e.g. xenon and krypton) and helium [17]. Hence, in the real spent fuel rod, a gap conductance (i.e. thermal contact resistance) exists between the fuel and the clad, and varies with irradiation history. To include the effects of gap conductance, we performed calculations for two cases: (1) assuming infinite gap conductance (i.e. no contact resistance) and (2) assuming the core and the fill gas have the same conductivity (i.e. neglecting the higher conductivity of the fuel). The second case is only for illustration purposes and a lower bound on F_{cond} can be determined by considering both $k_{core} \ll k_{fill}$ and $k_{core} \ll k_{tube}$ which is equivalent to assuming infinite

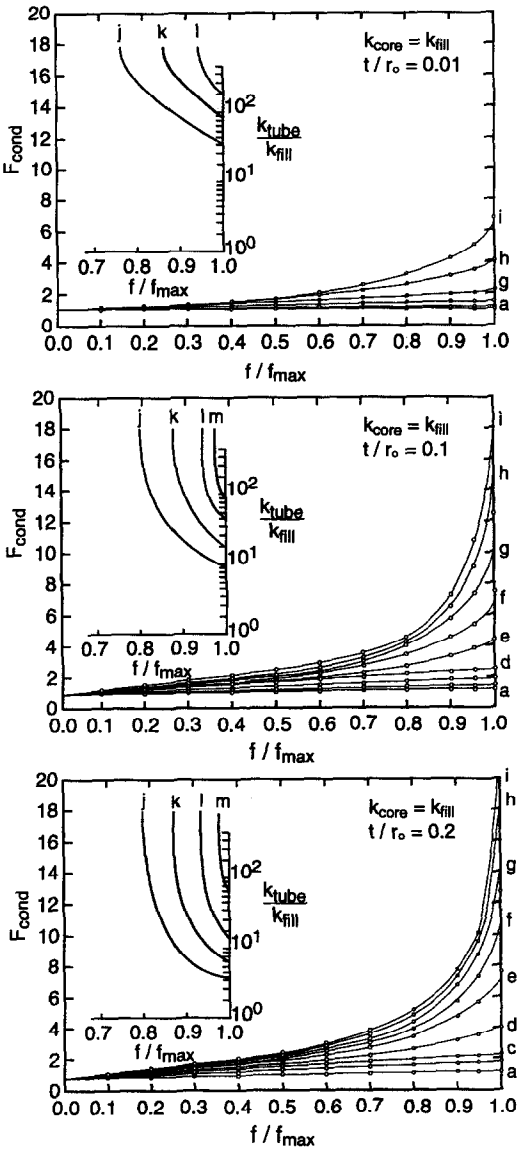

FIG. 6. Comparison of numerically calculated conduction factors (circles) with the 4th and 5th order analytic formulae (solid lines) for a square array of tubes k_{rod}/k_{fill} = for three tube wall thickness ratios, $t/r_o = \{0.01, 0.1, 0.2\}$ for nine rod-to-fill conductivity ratios, $k_{tube}/k_{fill} = \{1(a), 2(b), 5(c), 10(d), 20(e), 50(f), 100(g), 200(h), 10000(i)\}$. The percent error contours {0.01%(j), 0.1%(k), 1.0%(l), 10.0%(m)} are shown in the upper-left sub-plots.

gap resistance. However, this lower bound in not considered in this work. The analytic formulae and the numerical calculations are compared in Fig. 7 where calculations were performed for (1) square and hexagonal arrays; (2) nitrogen and helium back fill gas; (3) assuming both infinite gap conductance and $k_{core} = k_{fill}$. This resulted in eight analytic and eight numerical curves for comparison. Higher order analytic formula (4th & 5th order for the SQ array, 6th, 7th & 8th order for the HX array) were found to achieve excellent agreement with the numerical results

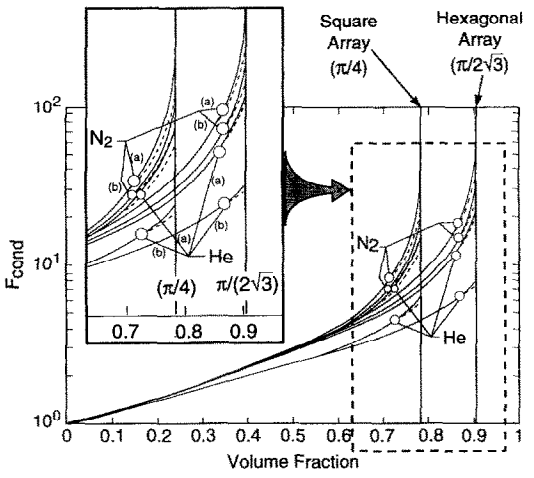

FIG. 7. Comparison of numerically calculated conduction factors (solid lines) with 4th & 5th order square array and 6th, 7th & 8th order hexagonal array analytic formulae (dashed lines) for spent nuclear fuel rods in either nitrogen or helium gas assuming either (a) infinite gap conductance or (b) $k_{core} = k_{fill}$.

at the higher volume fractions (see the dashed lines in Fig. 7).

For comparison, a typical PWR assembly has a square array and a rod pitch-to-diameter ratio of $p/d = 1.33$ which results in $f = 0.44$. For this case the analytic formulae are considered accurate. A consolidated assembly has a hexagonal array and a closer rod spacing ($0.75 < f < 0.9$), so that the higher-order analytic formulae are required for accuracy.

SUMMARY

A set of analytic formulae for the effective conductivity of either a square or hexagonal array of parallel tubes has been developed and numerically validated. In summary:

- The formulae are based on a generalization of Rayleigh's [9] method to include hexagonal (as well as square) arrays, tubes (as well as solid rods), and higher-order terms in the analytic series, see Table 1.
- The accuracy of the formulae was computed using essentially exact numerical calculations.
- The analytic formulae increasingly underestimate F_{cond} for increasing volume fraction and increasing rod-to-fill conductivity ratio, see Figs. 4 and 5.
- The accuracy of the formulae for the case of infinitely conducting (isothermal) solid rods was calculated and tabulated, see Tables 2 and 3.
- The analytic formulae were noted to be accurate for tubes ($k_{core} = k_{fill}$) as well as solid rods, see Fig. 6.
- For the case of dry, spent, nuclear fuel rods, the 4th & 5th order formula for the square array and the 6th, 7th & 8th order formula for the hexagonal array are considered accurate, see Fig. 7.

Acknowledgements—This work was originally performed at MIT with support by the U.S. Department of Energy through Sandia National Laboratories and under Contract No. DE-ACO4-76DP00789. Dr Manteufel is currently at Southwest Research Institute, where this paper was prepared with assistance under Contract No. NRC-02-88-005.

REFERENCES

1. G. S. Springer and S. W. Tsai, Thermal conductivities of unidirectional materials, *J. Composite Mater.* **1**(2), 166–173 (1967).
2. U. Tzadka and K. Schulgasser, Effective properties of fiber-reinforced materials, *ASME J. Appl. Mech.* **50**, 828–834 (1983).
3. Z. Hashin, Analysis of composite materials, *ASME J. Appl. Mech.* **50**, 481–505 (1983).
4. J. N. Israelachvili, R. A. Sammut and A. W. Snyder, Birefringence and dichroism of photoreceptors, *Vision Res.* **16**, 47–52 (1976).
5. J. N. Israelachvili, R. A. Sammut and A. W. Snyder, Birefringence and dichroism in invertebrate photoreceptors, *J. Optical Soc. Am.* **65**(2), 221–222 (1975).
6. W. T. Perrins, D. R. McKenzie and R. C. McPhedran, Transport properties of regular arrays of cylinders, *Proc. R. Soc. Lond., Series A* **369**, 207–225 (1979).
7. W. T. Perrins, R. C. McPhedran and D. R. McKenzie, Optical properties of dense regular cermets with relevance to selective solar absorbers, *Thin Solid Films* **57**, 321–326 (1979).
8. B. W. Ninham and R. A. Sammut, Refractive index of arrays of spheres and cylinders, *J. Theor. Biol.* **56**, 125–149 (1976).
9. Lord Rayleigh, On the influence of obstacles arranged in rectangular order upon the properties of a medium, *Phil. Mag.* **34**(5), 481–502 (see also *Scientific Papers by Lord Rayleigh*. Dover Publications, New York) (1892).
10. von I. Runge, Zur Elektrischen Leitfähigkeit Metallischer Aggregate, *Z. Technische Physik.* **6**(91), 61–68 (1925).
11. J. B. Keller, Conductivity of a medium containing a dense array of perfectly conducting spheres or cylinders or nonconducting cylinders, *J. Appl. Phys.* **34**(4), 991–993 (1963).
12. J. B. Keller, A theorem on the conductivity of a composite medium, *J. Math. Phys.* **5**(4), 548–549 (1964).
13. K. S. Mendelson, A theorem on the effective conductivity of a two-dimensional heterogeneous medium, *J. Appl. Phys.* **46**(11), 4740–4741 (1975).
14. H. Levine, The effective conductivity of a regular composite medium, *J. Inst. Math. Appl.* **2**, 12–28 (1966).
15. R. C. McPhedran, L. Poladian and G. W. Milton, Asymptotic studies of closely spaced, highly conducting cylinders, *Proc. R. Soc. Lond., Series A* **415**, 185–196 (1988).
16. R. D. Manteufel, Heat transfer in an enclosed rod array, Ph.D. Thesis, Massachusetts Institute of Technology, Cambridge, MA (1991).
17. N. E. Todreas and M. S. Kazimi, *Nuclear Systems I: Thermal Hydraulic Fundamentals*. Hemisphere, New York (1990).
18. *NEKTON User's Guide*. Nektonics, Inc., Cambridge MA (1990).

APPENDIX A: ANALYTICAL FORMULAE

The basic method is outlined by Rayleigh [9] and has been discussed by Perrins *et al.* [6, 7], among others. This discussion is presented to (i) provide new insights into the derivation, hence complement previous discussions, and (ii) give the interested reader the flavor of the derivation of the analytic solution. For example, the generalization to tubes is more fully developed as well as the distinctions

among linear, triangular and square truncations used in the development.

The analysis begins by considering a quarter cylinder in a square box as shown in Fig. A1. The temperature solution in the fill and rod regions are assumed to be of the form:

$$T_{\text{fill}} = \sum_{n=1,3,5,\ldots}^{\infty} \left(A_n r^n + \frac{B_n}{r^n}\right)\cos(n\theta) \tag{A1}$$

and

$$T_{\text{rod}} = \sum_{n=1,3,5,\ldots}^{\infty} C_n r^n \cos(n\theta). \tag{A2}$$

The origins of these expansions do not appear obvious, however, they are noted to satisfy the boundary conditions. In particular, the assumed temperature profiles satisfy the left (isothermal) boundary condition of:

$$T\left(r, \theta = \frac{\pi}{2}\right) = 0 \tag{A3}$$

and the bottom (insulated) boundary condition of:

$$\frac{\partial T}{\partial \theta}(r, \theta = 0) = 0. \tag{A4}$$

The expansions are also required to satisfy the interface boundary conditions:

$$T_{\text{fill}}(r = r_o, \theta) = T_{\text{rod}}(r = r_o, \theta) \tag{A5}$$

and

$$k_{\text{fill}} \frac{\partial T_{\text{fill}}}{\partial r}(r = r_o, \theta) = k_{\text{rod}} \frac{\partial T_{\text{rod}}}{\partial r}(r = r_o, \theta). \tag{A6}$$

The insertion of equations (A.1) and (A.2) into equations (A.5) and (A.6) leads to two equations with three sets of unknowns. The equations constrain two of the sets of variables (A's, B's, or C's) in terms of one of the sets of variables. For example, the A's and C's can be expressed as functions of the B's:

$$A_n = \frac{1}{v(r_o)^{2n}} B_n \tag{A7}$$

and

$$C_n = \frac{v}{(v+1)(r_o)^{2n}} B_n \tag{A8}$$

where

$$v = \frac{k_{\text{fill}} - k_{\text{rod}}}{k_{\text{fill}} + k_{\text{rod}}}. \tag{A9}$$

The solutions can then be expressed as functions of the unknown B's:

$$T_{\text{fill}} = \sum_{n=1,3,5,\ldots}^{\infty} B_n \left(\frac{r^n}{v(r_o)^{2n}} + \frac{1}{r^n}\right)\cos(n\theta) \tag{A10}$$

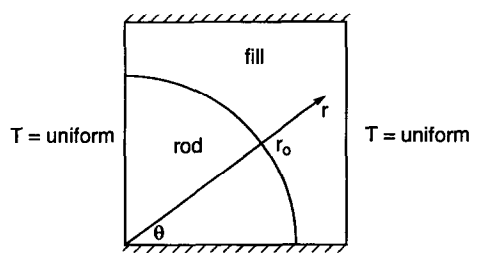

FIG. A1. Quarter cylinder considered in the derivation of the analytic formulae.

$$T_{\text{rod}} = \sum_{n=1,3,5,\ldots}^{\infty} B_n \left(\frac{1+v}{v}\right)\frac{r^n}{(r_o)^{2n}}\cos(n\theta). \tag{A11}$$

The B's are calculated using the method of Rayleigh which can be interpreted as enforcing the top (insulated) boundary condition and the right (isothermal) boundary condition. In addition, the values of the B's depend on the type of array considered. Here for example, a square array is considered. A hexagonal array would have the same structure as equations (A10) and (A11), however the B's would have different values. These two boundary conditions are only approximately satisfied and the agreement improves with more terms in the series. Rayleigh's method yields:

$$\delta_{n,1} - v\frac{B_{2n-1}}{(r_o)^{2n}} = \sum_{m=1,3,5,\ldots}^{M} \frac{(n+m-1)!}{n!(m-1)!} S_{n+m} B_m \tag{A12}$$

where n is odd and ranges from 1, 3, 5, ... up to N, and

$$\delta_{n,1} = \begin{cases} 1 & n = 1 \\ 0 & \text{otherwise} \end{cases}.$$

The parameter M in equation (A12) is determined from one of three options:

$$M = \begin{cases} \begin{cases} N & n = 1 \\ 1 & n > 1 \end{cases} & \text{Linear Truncation} \\ N - n + 1 & \text{Triangular Truncation} \\ N & \text{Square Truncation} \end{cases}.$$

The terms linear, triangular and square are used to indicate the shape of the set of equations generated on the right hand side of equations (A12) through the choice of M. The linear truncation indicates that only one term is on the right hand side for each equation after the first. The square truncation indicates that each equation (from first to last) has the same number of terms on the right hand side. The triangular truncation has decreasingly fewer terms on the right hand side for increasing N (i.e. the number of equations). The 'linear' truncation was used by Rayleigh [9] and the 'triangular' truncation has been used by Perrins *et al.* [6, 7], among others. Similarly, the 'square' truncation has been discussed by Perrins *et al.* [6]. Equation (A12) generates a set of N equations in N unknowns which can be solved to yield the B's. The S's in equation (A12) are numerical coefficients which can be calculated from a summation of the form:

$$S_k = \sum_{j=1}^{\infty} (x_j + \sqrt{(-1)}y_j)^{-k} \tag{A13}$$

where (x_j, y_j) are the locations of all of the surrounding cylinder centers (excluding the cylinder at the origin). The values of the S's have been calculated for the square array:

$$\begin{aligned} S_2 &= \pi = 3.1415926 \\ S_4 &= 3.1512112 \\ S_8 &= 4.2557732 \\ S_{12} &= 3.9388490 \\ S_{16} &= 4.0156950 \\ S_{20} &= 3.9960967 \\ S_{24} &= 4.0009768 \\ S_{28} &= 3.9997559 \\ S_{32} &= 4.0000610 \\ S_{36} &= 3.9999847 \\ S_{40} &= 4.0000038 \\ S_{44} &= 3.9999990 \\ S_{48} &= 4.0000002 \\ S_{52} &= 3.9999999 \end{aligned}$$

and for the hexagonal array:

$$S_2 = \frac{2\pi}{\sqrt{(3)}} = 3.6275987$$
$$S_6 = 5.8630317$$
$$S_{12} = 6.0096400$$
$$S_{18} = 5.9997184$$
$$S_{24} = 6.0000116$$
$$S_{30} = 5.9999996$$
$$S_{36} = 6.0000000.$$

The effective conductivity can be calculated using Green's Theorem with the solutions for the temperature distributions. This yields:

$$F_{\text{cond}} = 1 - 2\pi B_1. \tag{A14}$$

The procedure is to solve the equations generated by equation (A12) for B_1 and substitute the solution into equation (A14). The 'order' of the analytic series is determined by the choice of 'N' in equation (A12). In Table 1 of this paper, the analytic solutions were generated using the 'triangular' truncation scheme with $N = 1, 2, \ldots, 7$ for the square array, and with $N = 1, 2, \ldots, 11$ for the hexagonal array. The reader is reminded that for the square array the solutions are equal for sets of N (i.e. $N = (2 \text{ or } 3)$ generate the same solution, $N = (4 \text{ or } 5)$ generate the same solution, $N = (6 \text{ or } 7)$ generate the same solution). Similarly, for the hexagonal array the solutions are the same when $N = (3 \text{ or } 4 \text{ or } 5)$, $N = (6 \text{ or } 7 \text{ or } 8)$, and $N = (9 \text{ or } 10 \text{ or } 11)$. These groupings of solutions are shown in Table 1 and throughout this paper.

The generalization to tubes is considered straightforward where three temperature distributions are assumed as shown (compare with equations (A1) and (A2):

$$T_{\text{fill}} = \sum_{n=1,3,5,\ldots}^{\infty} \left(A_n r^n + \frac{B_n}{r^n}\right)\cos(n\theta) \tag{A15}$$

$$T_{\text{tube}} = \sum_{n=1,3,5,\ldots}^{\infty} \left(C_n r^n + \frac{D_n}{r^n}\right)\cos(n\theta) \tag{A16}$$

and

$$T_{\text{core}} = \sum_{n=1,3,5,\ldots}^{\infty} E_n r^n \cos(n\theta). \tag{A17}$$

The edge boundary conditions remain the same (equations (A3) and (A4)). The interior boundary conditions are as shown (compare with equations (A5) and (A6)):

$$T_{\text{fill}}(r = r_o, \theta) = T_{\text{tube}}(r = r_o, \theta) \tag{A18}$$

$$k_{\text{fill}} \frac{\partial T_{\text{fill}}}{\partial r}(r = r_o, \theta) = k_{\text{tube}} \frac{\partial T_{\text{tube}}}{\partial r}(r = r_o, \theta) \tag{A19}$$

$$T_{\text{tube}}(r = r_i, \theta) = T_{\text{core}}(r = r_i, \theta) \tag{A20}$$

and

$$k_{\text{tube}} \frac{\partial T_{\text{tube}}}{\partial r}(r = r_i, \theta) = k_{\text{core}} \frac{\partial T_{\text{core}}}{\partial r}(r = r_i, \theta). \tag{A21}$$

The four constraints can be used to express four of the unknown sets of variables (e.g. A's, C's, D's, and E's) in terms of one of the sets of variables (e.g. B's). The temperature fields can both be expressed in terms of only the B's. An equation similar to equation (A12) can be established where the v's are generalized to be a function of n as shown:

$$v_n = \frac{\delta_{\text{fill-tube}} + \delta_{\text{tube-core}}\left(\frac{r_i}{r_o}\right)^{2n}}{1 + \delta_{\text{fill-tube}}\delta_{\text{tube-core}}\left(\frac{r_i}{r_o}\right)^{2n}}. \tag{A22}$$

APPENDIX B: NUMERICAL CALCULATIONS

The array conduction factors were numerically calculated using the four elemental volumes shown in Figs. B1 and B2. One-dimensional heat transfer is assumed in the 0° and 45° directions for the square array, and in the 0° and 30° directions for the hexagonal array. The isothermal and adiabatic boundary conditions are indicated in Figs. B1 and B2 of this paper. In each elemental volume, three distinct regions are illustrated: core, tube and fill. The heat conduction equation applies for each region, i.e. grad $(T) = 0$. The interface between adjacent regions is assumed to be locally isothermal (i.e. thermal contact resistance is not considered).

The elemental volumes in Figs. B1 and B2 are the most fundamental volumes which take advantage of both the thermal and geometrical symmetry. The square array is geometrically symmetric every 90° rotation, and a 45° rotation introduces a distinct direction. The hexagonal array is symmetric every 60° rotation, and a 30° rotation introduces a distinct direction. To simulate a solid rod, the core and tube conductivities are set to be equal. To simulate a hollow tube, the core and fill conductivities are set to be equal (the term hollow tube is consistent with Runge [10]).

A commercially available computer program called NEKTON [18] was used. The domains were discretized into 'macro' elements as shown in Figs. B1 and B2. For example, the horizontal volume from the square array was discretized into seven macro elements where three were for the core, two for the tube and two for the fill. One extra

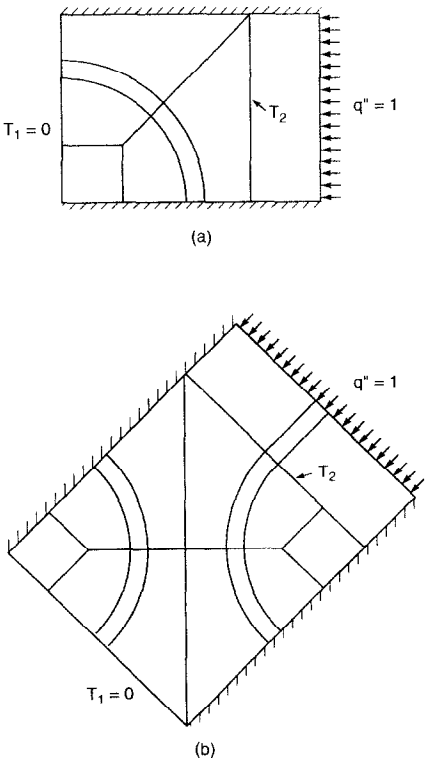

FIG. B1. Spectral element mesh used to calculate the conduction factor for a square array in the (a) horizontal and (b) 45 degree direction.

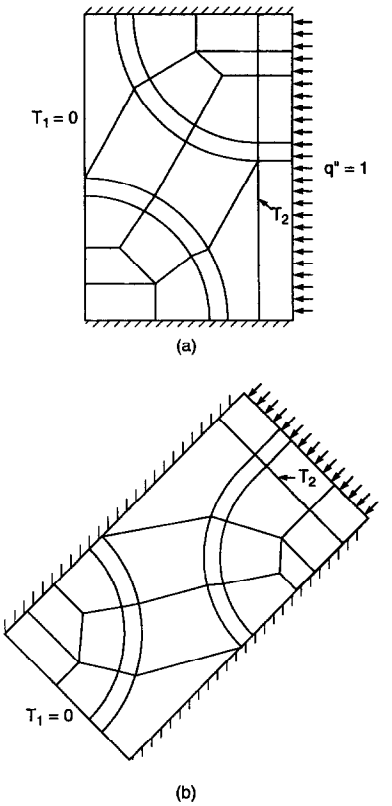

FIG. B2. Spectral element mesh used to calculate the conduction factor for a hexagonal array in the (a) horizontal and (b) 30 degree direction.

element was added as an isothermal element (conductivity 1000 times larger than the fill conductivity) for computational convenience. In total, eight macro elements were used to discretize the domain in Fig. B1(a). NEKTON is a spectral element computer program which allows high-order discretization. Both 5×5 and 7×7 polynomial tensor products were used in each macro element. The results were compared for varying p/d and both were found to yield essentially the same solution (to approximately five significant digits in F_{cond}). This comparison of 5×5 and 7×7 results confirmed numerical convergence and a 7×7 discretization was used for all of the results. Tables of results are presented by Manteufel [16].

A heat flux was specified on one side of the isothermal element which then acted as an isothermal boundary condition. The conduction factor was determined by the discrete form of Fourier's law:

$$q'' = F_{cond} k_{fill} \left(\frac{T_2 - T_1}{L} \right) \tag{B1}$$

where

q'' = heat flux [W m^{-2}]
F_{cond} = conduction factor [dimensionless]
k_{fill} = fill conductivity [W m^{-1} °C^{-1}]
L = length between isothermal boundaries [m]
T_2 = temperature [°C], and
T_1 = temperature [°C].

The lengths can be related to the pitch (distance from rod center to rod center):

$$L = \begin{cases} \frac{1}{2}p & \text{Fig. B1(a)} \\ \frac{\sqrt{2}}{2}p & \text{Fig. B1(b)} \\ \frac{1}{2}p & \text{Fig. B2(a)} \\ \frac{\sqrt{3}}{2}p & \text{Fig. B2(b).} \end{cases}$$

The fill conductivity, total heat flux and right side temperature are specified as $k_{fill} = 1.0$ W m^{-1} °C^{-1}, $q'' = 1.0$ W m^{-2}, and $T_1 = 0.0$°C. The maximum temperature, T_2, is then calculated using NEKTON. The additional high conductivity element was used for computational convenience because the heat flux is not necessarily uniform while the temperature T_2 is uniform along the left side edge of the mesh. By introducing the high conductivity element, the uniform temperature was ensured while the applied heat flux automatically adjusted in the solution. The conduction factor is then calculated using:

$$F_{cond} = \left(\frac{L}{T_2} \right) \tag{B2}$$

where T_2 is calculated by the computer program.